OPEN ACCESS
ARTICLE

Single-Step Synthesis of $LaMnO_3$/MWCNT Nanocomposites and Their Photocatalytic Activities

Regular Paper

Hao Huang[1], Guangren Sun[1], Jie Hu[1,2*] and Tifeng Jiao[2,3*]

1 State Key Laboratory of Metastable Materials Science & Technology, Yanshan University, Qinhuangdao, P.R. China
2 Hebei Key Laboratory of Applied Chemistry, School of Environmental and Chemical Engineering, Yanshan University, Qinhuangdao, P.R. China
3 National Key Laboratory of Biochemical Engineering, Institute of Process Engineering, Chinese Academy of Sciences, Beijing, P.R. China
* Corresponding author(s) E-mail: hujie@ysu.edu.cn; tfjiao@ysu.edu.cn.

Received 17 June 2014; Accepted 28 August 2014

DOI: 10.5772/59063

Abstract

Composites of the nano-sized perovskite-type oxide of $LaMnO_3$ and multi-walled carbon nanotubes (MWCNTs) were synthesized in a single step using the sol-gel method. Their photocatalytic activities for the degradation of various water-soluble dyes under visible light were evaluated. The prepared samples were characterized by thermogravimetry analysis, scanning electron microscopy, transmission electron microscopy, X-ray diffraction, photoluminescence spectroscopy and UV-vis diffused spectroscopy. Results showed that $LaMnO_3$ nanoparticles grew on the surface of MWCNTs with a grain size of around 20 nm. Photocatalysis measurements revealed that the $LaMnO_3$/MWCNT nanocomposites had greater photocatalytic activities than pure $LaMnO_3$ nanoparticles, and the mass percentage of MWCNTs showed that 9.4% possessed the highest photocatalytic activity. These results indicate that $LaMnO_3$/MWCNT nanocomposites are promising candidates as highly effective photocatalysts.

Keywords Carbon nanotubes, Nanocomposites, Perovskite-type structure, Photocatalysis

1. Introduction

Carbon nanotubes (CNTs), one of the most important materials in the 21st century technology, are regarded as representatives for nanotechnology. They possess uniquely extraordinary structural, electronic, chemical and physical properties, with broad potential applications in various industries such as electrodes, nanoelectronic devices, chemical sensors and optoelectronic applications [1-3]. Currently, there has been widespread interest in the fabrication of one-dimensional nanoscale materials by coating CNTs with various kinds of materials including metals, non-metals, carbides and oxides [4]. Recently, the attachment of various metal oxides onto the CNT substrate, including SiO_2, SnO_2, Fe_3O_4, TiO_2, ZnO and Al_2O_3, has been reported [5-10]. However, so far, relatively little attention has been paid to perovskite/CNT nanocomposites.

In recent years, with increasing environmental pollution, the degradation of organic pollutants has aroused broad interest in the study of photo-catalysis for both scientific understanding and potential applications [11-15]. Solar energy, an abundant natural energy source, can be widely

utilized in the photo-catalytic degradation of pollutants [16-17]. A large number of studies have shown that photocatalytic oxidation plays an important role on the removal of dyes from waste water, which contains direct dyes, sulphur dyes, reactive dyes, acid dyes and other components. Among these oxides, as some of the promising photocatalysts, perovskite-type oxides have been widely researched because of their low cost, simple preparation, high photochemical stability and friendliness towards the environment. However, the utilization of perovskite-type oxides as photocatalysts has practical limitations, such as the fast electronhole recombination that reduces the efficiency. In fact, the low quantum yield (about 4%) hinders the further application of perovskite-type oxides [18].

Many efforts have been devoted to improve the separation efficiency of light induced e--h^+, broaden the absorption edge and increase surface reactions for perovskite-type oxide [19-21]. The main way of inhibiting the reunion of light induced e--$h^+$is to facilitate the transportation of holes or electrons by doping with a cation to perovskite-type oxide and the method of accelerating surface reactions is supporting perovskite-type oxides with materials that have excellent adsorption ability [22].

As an important perovskite-type structure photocatalyst, $LaMnO_3$ has been applied for the photocatalytic production of hydrogen from water and degradation of organic pollutants under UV-Vis light irradiation. Maryam et al. [23] studied that the photocatalytic activity of $LaMnO_3$ by degradation of methyl orange in an aqueous solution under visible-light irradiation. Naidu et al. [24] reported a study of the visible light induced oxidation of water by perovskite oxides of the formula $LaMO_3$ (M=transition metal), revealed that among the rare earth manganites, only orthorhombic manganites with octahedral Mn^{3+}ions exhibit good catalytic activity.

In this work, one-step synthesis of $LaMnO_3$/MWCNT nanocomposite powders were carried out using the sol-gel method and the photocatalytic capabilities of composites were investigated under visible light. In contrast to pure perovskite-type oxide, synergistic effects were observed for the composite in the degradation of some organic dyes due to the electron scavenger role of MWCNTs in the composite, which helped to enhance e^--h^+separation [25]. Moreover, this implicated that MWCNTs in the composite could help concentrate organic dyes on the composite surface, enhancing the photocatalytic degradation rate.

2. Experimental

2.1 Preparation of catalysts

MWCNTs used for the present work were purchased from Shen Zhen Nanoharbor Limited and produced by catalytic hydrocarbon decomposition. These MWCNTs have a mean outer diameter of 30 nm and a length of 1 μm. In a typical procedure, 0–75 mg MWCNTs were dispersed in 100 mL ethanol solution, which were ultrasonicated for one hour, and the pH level was adjusted to ~9 using aqueous ammonia. $La(NO_3)_3$ (0.002 mol) and $Mn(NO_3)_2$ (0.002 mol) were subsequently dissolved into the suspension. To establish the stoichiometric ratio for the solution, citric acid was successively added (at a molar ratio of 2:1 with respect to the cations) and complexed with metal ions in nitrate to form the stable complex sol.

Citric acid is a ternary carboxylic acid steady compound which can be formed by adjusting pH of solution. When pH is 9, following this reaction: $La^{3+}+Mn^{3+}+2(Cit)^{3-}\rightarrow$ [La Mn $(Cit)_2$].

The surface active agent octyl phenol polyoxyethylene ether-10 (Zibo Haijie Chemical Company) was added at a mass ratio of 3:20 with respect to the two nitrates to reduce the capillary force during the gel drying process and prevent the gel from cracking. Each step was accompanied by constant magnetic stirring. The mixture was then heated at 60°C to initiate the polymerization reaction, and the sol particles were adsorbed onto the surface of MWCNTs by weak interaction. The formed gel was dried at 80°C for 24 hours in a thermostat drier. The obtained xerogel was initially calcined at 450°C for two hours in air and then at 600°C for three hours in a vacuum to produce samples [22]. These samples were designated as x mg-$LaMnO_3$/MWCNT, where x denotes the corresponding concentration of the MWCNTs suspension.

2.2 Characterizations

The structure, morphology and composition of the synthesized powders were examined with a D/max–2500/pc X-ray diffractometer (Cu Kα radiation λ=1.5405 Å), field-emission scanning electron microscopy (FESEM, S-4800) and transmission electron microscopy (TEM, JEOL-2010) with an accelerating voltage of 200 kV. Furthermore, in order to examine the mass percentage of MWCNTs in the $LaMnO_3$/MWCNT nanocomposites, thermogravimetry (TG) experiments (STA 449C, NETZSCH, SELB, Germany) were carried out at a heating rate of 5ºC/min from 20 to 800°C in air. The Fluorescence emission spectra were obtained using a Hitachi F-4600 Spectrophotometer with a xenon laser, the excited wavelength of $LaMnO_3$ is 394 nm with a scanning intensity of 400 V. The UV-vis diffuse reflection spectra (DRS) were recorded with a Shimadzu UV-2550 spectrophotometer from 200 nm to 800 nm, the band gap energy was calculated using the following equation:

$$(Ahv)^2 = k(hv - Eg)$$

where A is the absorbance, k is the parameter related to the effective masses associated with the valence and conduction bands, n is equal to two for indirect transition, hv is the absorption energy, and Eg is the band gap energy. Accord-

ing to the DRS spectra, the band gap energy of $LaMnO_3$ is 2.67 *eV*

2.3 Photocatalytic experiments

The photocatalytic activities of the as-prepared $LaMnO_3$/MWCNT nanocomposites were investigated by the degradation of acid red (AR), methyl orange (MO), weak-acid yellow (WAY), direct green (DG) and methylthionine blue (MB) under the radiation of a 300 W xenon lamp (CHF-XM-300W, with a wavelength scope at 190-1100 nm, Beijing Trusttech Co. Ltd.). To make sure that the photocatalytic reaction was driven by visible-light, all the UV lights with a wavelength lower than 410 nm were removed by a glass filter. The initial dye concentration was 20 mg/L. The distance between the light source and liquid surface was approximately 20 cm. During this measurement of photocatalysis, 15 mg of photocatalysts was added to 100 mL of dye aqueous solution. Before illumination, the mixed solution was magnetically stirred for 30 minutes in the dark to obtain adsorption-desorption equilibrium. At 30 minute intervals, 5 mL of suspension was continually collected from the reaction cell and separated by centrifugation at 3000 rpm for five minutes. The absorption spectrum of the centrifuged solution was then measured. The degradation percentage of the dye was defined as $(C_0-C_t)/C_0\times100$, where C_0 and C_t are the dye concentrations before and after irradiation, respectively. For comparison, the photodecomposition experiments of dyes after irradiating for 48 hours without photocatalysts were observed under the same conditions.

3. Results and discussion

A relatively easier method was adopted to estimate the mass percentage of MWCNTs in the $LaMnO_3$/MWCNT nanocomposites. Fig. 1 shows the TG curves of raw MWCNTs and the calcined 50 mg-$LaMnO_3$/MWCNT sample. As can be seen from Fig. 1, the MWCNTs were oxidized beginning at 600°C or so, up to about 750°C, nearly the entire MWCNTs sample burned up with a residual mass of 1.57%, which was due to some residue impurities. The TG curve of 50 mg-$LaMnO_3$/MWCNT showed, at the temperature up to 750ºC, the residual mass was about 90.58%. According to the residual mass of $LaMnO_3$ and impurities (90.58%), the mass of $LaMnO_3$ was estimated to be 90.43%. Therefore, the mass percentage of MWCNTs in the 50 mg-$LaMnO_3$/MWCNT nanocomposites determined by TG was about 9.4.

The XRD spectra of the $LaMnO_3$ and 50 mg-$LaMnO_3$/MWCNT are shown in Fig. 2. Notably, the pattern of $LaMnO_3$ was consistent with that of PDF33–0713, indicating a perovskite-type structure with a complete crystal shape. The main strong lines of $LaMnO_3$ were obvious in both pure $LaMnO_3$ and $LaMnO_3$/MWCNT. After introducing MWCNTs to $LaMnO_3$ for photocatalysis, the XRD pattern revealed dispersed small peaks. This phenomenon may be due to the markedly smaller particle sizes of $LaMnO_3$ in $LaMnO_3$/MWCNT composites than those of pure $LaMnO_3$. The weak bands at the positions 2θ=27.76° and 45.84° could be respectively indexed as (002) and (100) crystal planes. The diffractions (PDF 41–1487) that were characteristic of MWCNTs corresponded with the graphitic nature of the MWCNTs [26]. The above analysis showed that the $LaMnO_3$/MWCNT nanocomposites had a two-phase structure and a perovskite-type structure as the main crystalline phase. With MWCNTs as carrier, the $LaMnO_3$ particles showed nucleation and growth.

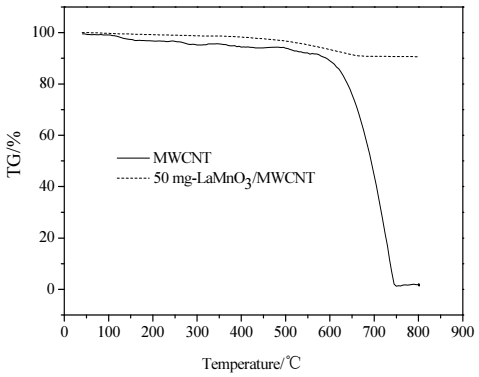

Figure 1. TG curves of raw MWCNTs and the calcined 50 mg-$LaMnO_3$/MWCNT sample

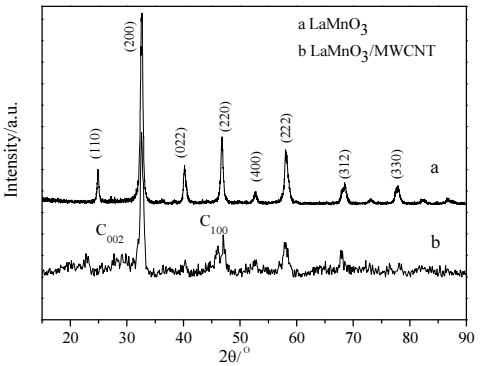

Figure 2. XRD patterns of $LaMnO_3$ and 50 mg-$LaMnO_3$/MWCNT

The morphologies of 50 mg-$LaMnO_3$/MWCNT are shown in Fig. 3. As shown in Fig. 3a and 3b, the nano-sized $LaMnO_3$ particles were well dispersed and deposited on the surface of MWCNTs, and the thickness was approximately 35 nm because of the purchased MWCNTs having a mean outer diameter of 30 nm. Electron diffraction patterns were also shown in Fig. 3c, in which there were two sets of lattice that were derived from $LaMnO_3$ and MWCNTs, respectively. Fig. 3d shows the HRTEM image of $LaMnO_3$/MWCNT. $LaMnO_3$ exhibited the interlayer spacing,

0.28nm, corresponding to (200) crystal planes, while MWCNTs corresponding to (002) and the interlayer spacing was 0.33 nm. As shown in Fig. 3d, the lattice structure of $LaMnO_3$ and MWCNTs were very orderly. It indicated that there was no change in the lattice structure of $LaMnO_3$ and MWCNTs after they were compounded.

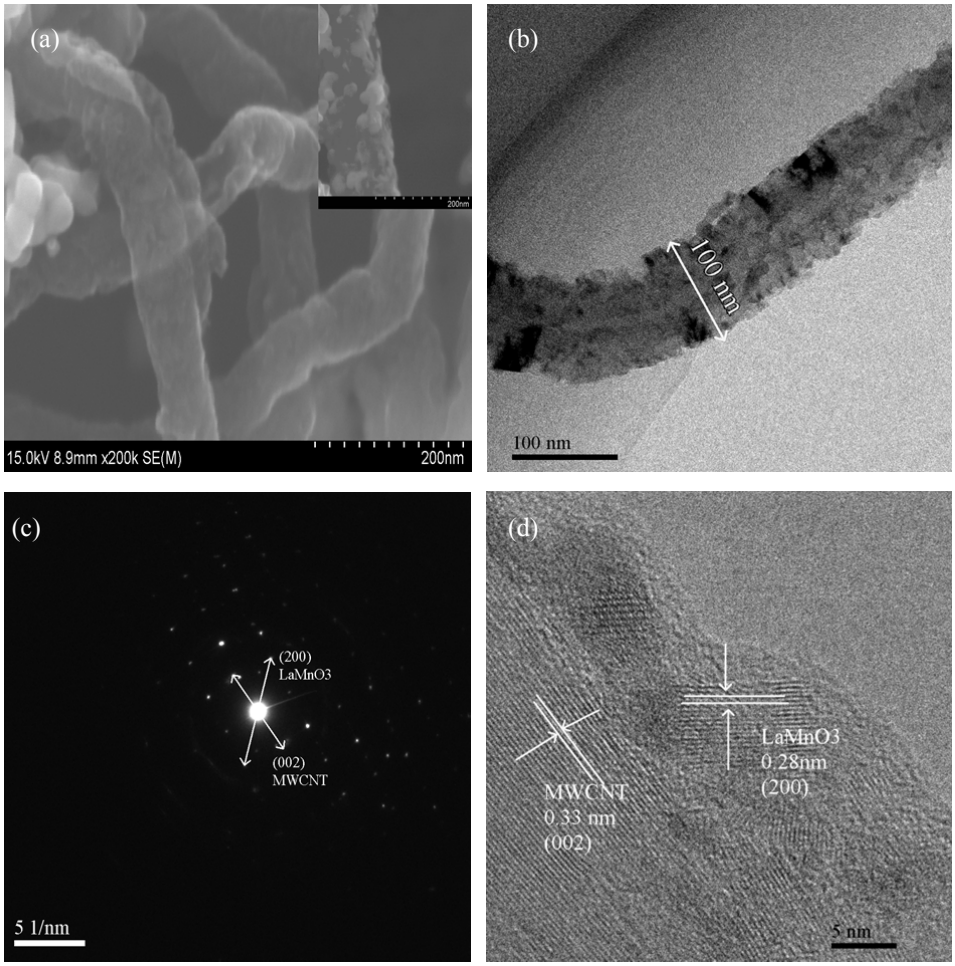

Figure 3. (a) SEM, (b) TEM, (c) SAED and (d) HRTEM images of 50 mg-$LaMnO_3$/MWCNT

The photocatalytic activities of different samples were studied by analysing the photodegradation of DG as a model reaction, and the results are shown in Fig. 4a. Fig. 4b showed the photocatalytic activities of different dyes by using a 50 mg-$LaMnO_3$/MWCNT sample. It can be seen from Fig. 4c and 4d, the photocatalytic degradation process is in accordance with the first-order kinetics.

Fig. 5a shows that DG dye has absorption peaks at 323, 395 and 625 nm. After three hours of exposure to light using $LaMnO_3$ as a photocatalyst, the peak absorption intensity of dye dramatically weakened, dropping from the initial 0.4144 to 0.1597. Under the same conditions, using 25 mg-$LaMnO_3$/MWCNT as the photocatalyst, the absorption peak intensity of dye was further reduced, indicating that 25 mg-$LaMnO_3$/MWCNT had better photocatalytic ability than pure $LaMnO_3$. After using 50 mg-$LaMnO_3$/MWCNT as the photocatalyst and irradiating for three hours, the UV-vis absorbance spectra were almost a straight line. However, the catalytic performance decreased with an increased amount of MWCNTs, due to the excess MWCNTs that covered the surface of $LaMnO_3$, obstructed the photons absorption.

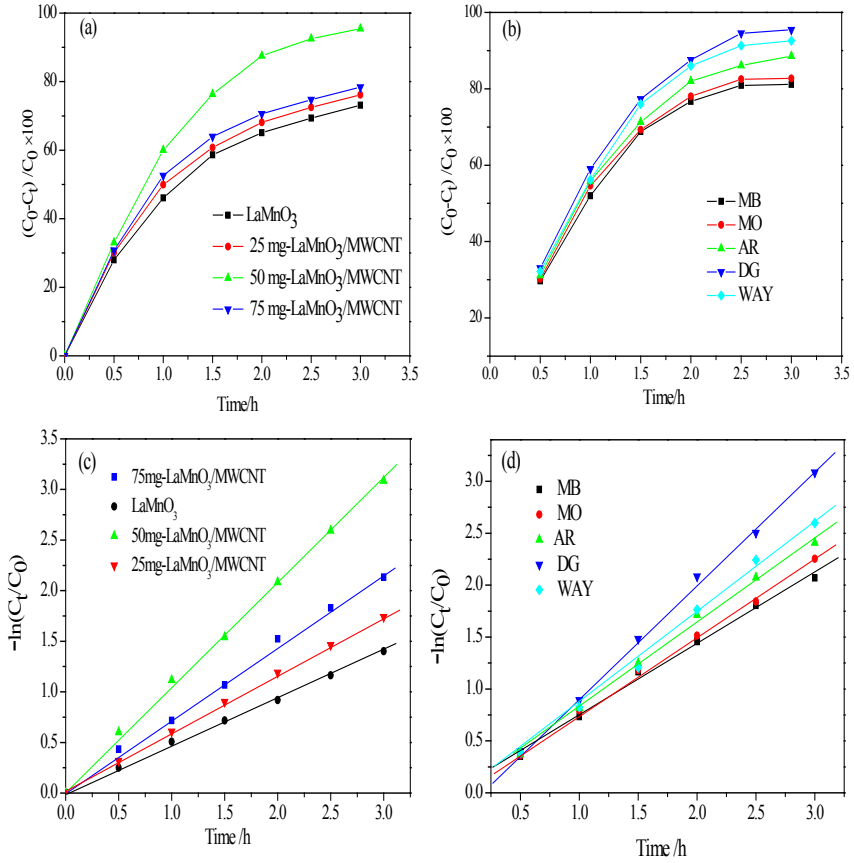

Figure 4. (a) Degradation percentages and (c) kinetics of photocatalytic degradation of DG by different samples, (b) Degradation percentages and (d) kinetics of photocatalytic degradation of different dyes by 50mg-$LaMnO_3$/MWCNT

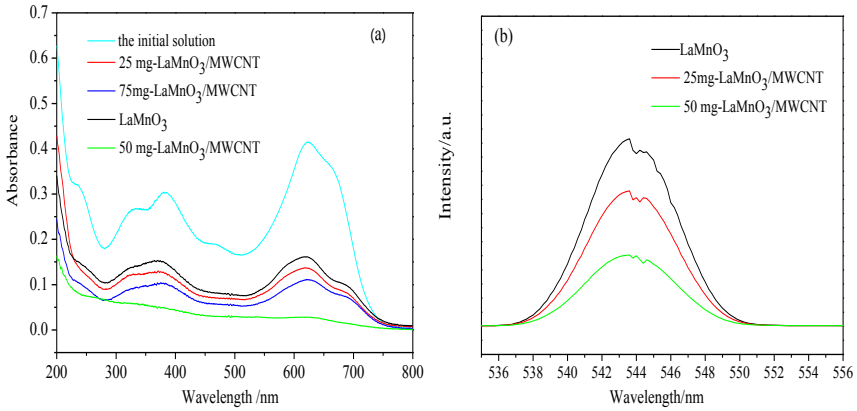

Figure 5. (a) UV–Vis spectral changes of the degradation of DG by different samples, (b) Fluorescence emission spectra of different samples

Fig. 5b displays the PL spectra of different samples. Previous studies had indicated that fluorescent emission spectra were the composite results of electron-hole pairs. The lower fluorescence emission intensity suggested the recombine rate was slower and the separation of photogenerated electrons and holes were more effective [27]. The $LaMnO_3$ sample appeared to have higher fluorescence intensity than that of $LaMnO_3$/MWCNT samples, which suggested that the compound for $LaMnO_3$ and MWCNTs could reduce the photogenerated electron-hole recombination rate. The 50 mg-$LaMnO_3$/MWCNT sample had the lowest fluorescence intensity, which was consistent with the aforementioned UV–Vis spectra.

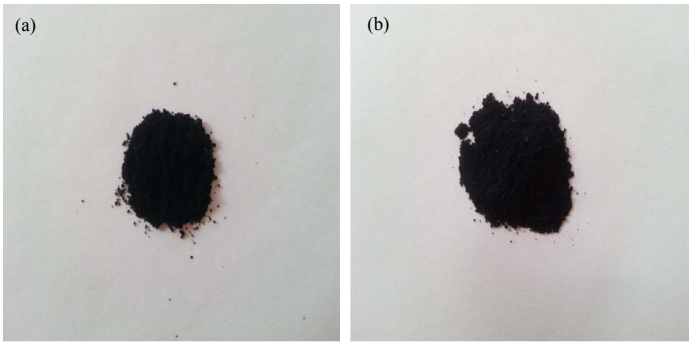

Figure 6. Pictures of $LaMnO_3$ and 50 mg-$LaMnO_3$/MWCNT

Fig. 6 shows the pictures of $LaMnO_3$ and 50 mg-$LaMnO_3$/MWCNT. It can be seen that the prepared samples are both in black, powder form.

The greater photocatalytic activity of the $LaMnO_3$/MWCNT nanocomposite than that of pure $LaMnO_3$ can be explained as follows. First, compared with pure $LaMnO_3$, the introduction of MWCNTs expanded the light response range and significantly increased the optical absorption of $LaMnO_3$ [28], thereby enhancing the photocatalytic activity. As shown in Fig. 7, the light absorption of 50 mg-$LaMnO_3$/MWCNT was significantly greater than that of $LaMnO_3$. An obvious red shift of about 34 nm was observed on the absorption edge of $LaMnO_3$/MWCNT nanocomposites. Second, the synergistic effect of MWCNTs and $LaMnO_3$ improved the photocatalytic quantum efficiency of $LaMnO_3$. $LaMnO_3$ particles were highly dispersed on the surface of MWCNTs, fully exposed to the photon irradiation of the illuminant, so as to facilitate the photons absorption. The special structure of MWCNTs was propitious to photogenerated electron transport within the scope of whole structure, thus reducing its recombination rate with photogenerated holes that went by the name of ballistic transport [29]. Finally, the perfect texture properties played an important role on improving the photocatalytic activity. The compound inhibited the aggregation of nanoparticles and the three-dimensional pore structure of composites could reduce the resistance to the mass transfer reaction process, thus allowing the pollutant molecules to more easily transfer close to the active site and improve the photocatalytic activity.

Fig. 8 shows the degradation percentages of the dyes after irradiation for three hours using $LaMnO_3$ and 50 mg-$LaMnO_3$/MWCNT. As shown in Fig. 8, the blank measurements were the photodecomposition effect of dyes after irradiating for 48 hours without photocatalysts. Compared with $LaMnO_3$, the 50 mg-$LaMnO_3$/MWCNT exhibited higher photocatalytic activity for the degradation of the five dyes, which proved that $LaMnO_3$/MWCNT composites were highly effective photocatalysts for dye degradation. It can be seen that the degradation rate had a dependence on the type of dye, and DG exhibited the highest degradation efficiency among the five dyes. Numerous factors were expected to collectively contribute to the differences between the degradation rates of the dyes, such as the dye adsorption properties of the catalyst particles and the molecular structure of the dye. The exact mechanisms involved need further investigation [30].

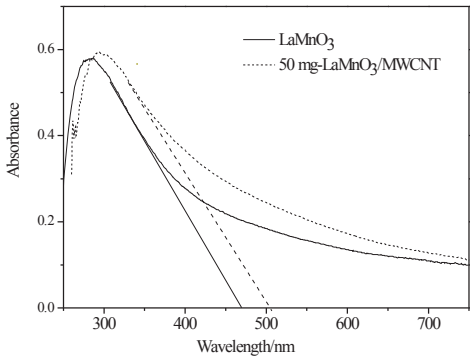

Figure 7. UV–vis DRS spectra of $LaMnO_3$ and 50 mg-$LaMnO_3$/MWCNT

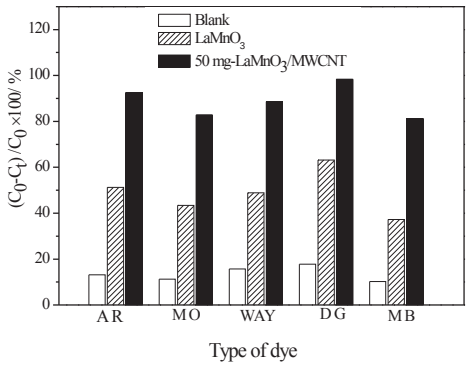

Figure 8. Dye degradation percentages after three hours of irradiation using $LaMnO_3$ and 50 mg-$LaMnO_3$/MWCNT

4. Conclusion

$LaMnO_3$/MWCNT nanocomposites were synthesized in a single step by the sol-gel method, and their photocatalytic performances were tested by various water-soluble dyes degradation under visible light irradiation. A pure $LaMnO_3$ perovskite-type structure phase was successfully anchored onto the surface of MWCNTs, and $LaMnO_3$/MWCNT nanocomposites exhibited excellent photocatalytic activity than that of conventional $LaMnO_3$ nanoparticles. These results can serve as a foundation for further research on developing MWCNTs-hybridized materials and improving the photocatalytic activity of the perovskite-type structure photocatalyst.

5. Acknowledgements

The authors gratefully acknowledge the support of the Research Program of the College of Science & Technology of Hebei Province (No. QN20131026), and the Technology Support Program of Hebei Province (No. 13214903). This work is also financially supported by the National Natural Science Foundation of China (Nos. 21473153 and 51402253), Natural Science Foundation of Hebei Province (No. B2013203108), Science Foundation for the Excellent Youth Scholars from Universities and Colleges of Hebei Province (No. YQ2013026), Support Program for the Top Young Talents of Hebei Province, and Open Foundation of National Key Laboratory of Biochemical Engineering, Institute of Process Engineering of Chinese Academy of Sciences.

6. References

[1] Jiang G, Wang L, Chen C, Dong X, Chen T, Yu H (2005) Attachment of Branched Molecules on Multiwalled Carbon Nano-Tubes. Mater. Lett. 59: 2085-2089.

[2] Zhu L, Sun Y, Hess D W, Wong C P (2006) Well-Aligned Open-Ended Carbon Nanotube Architectures: an Approach for Device Assembly. Nano Lett. 6: 243-247.

[3] Hamadanian M, Jabbari V, Shamshiri M, Asad M Mutlay, I (2013) Preparation of Novel Hetero-Nanostructures and High Efficient Visible Light-Active Photocatalyst Using Incorporation of CNT as An electron-Transfer Channel into the Support TiO_2 and PbS. J. Taiwan Inst. Chem. E. 44: 748-757.

[4] Lu J, Zang J B, Shan S X, Huang H, Wang Y H (2008) Synthesis and Characterization of Core-Shell Structural MWCNT-Zirconia Nanocomposites. Nano Lett. 11: 4070-4074.

[5] Cho J, Schaab S, Roether A J, Boccaccini A R (2008) Nanostructured Carbon Nanotube/TiO_2 Composite Coatings Using Electrophoretic Deposition. J. Nanopart. Res. 10: 99-105.

[6] Jiang L Q, Gao L (2005) Fabrication and Characterization of ZnO-Coated Multi-Walled Carbon Nanotubes with Enhanced Photocatalytic Activity. Mater.Chem. Phys. 91: 313-316.

[7] Korneva G, Ye H H, Gogotsi Y, Halverson D, Friedman G, Bradley J C, Kornev K G (2005) Carbon Nanotubes Loaded with Magnetic Particles. Nano Lett. 5: 879-885.

[8] Kauffman D R, Tang Y, Kichambare P D, Jackovitz J F, Star A (2010) Long-Term Performance of Pt-Decorated Carbon Nanotube Cathodes in Phosphoric Acid Fuel Cells. Energ. Fuel. 24: 1877-1881.

[9] Han W, Zettl A (2003) Coating Single-Walled Carbon Nanotubes with Tin Oxide. Nano Lett. 3: 681-683.

[10] Sun J, Gao L, Li W (2002) Colloidal Processing of Carbon Nanotube/Alumina Composites. Chem. Mater. 14: 5169-5173.

[11] Arthur J, Esswein, Daniel G (2007) Nocera Hydrogen Production by Molecular Photocatalysis. Chem. Rev. 107: 4022-4047.

[12] Masakazu A, Masato T (2003) The Design and Development of Highly Reactive Titanium Oxide-photocatalysts Operating Under Visible Light Irradiation. J. Catal. 216: 505-516.

[13] Pillai S C, Periyat P, George R, McCormack D E, Seery M K, Hayden H, Colreavy J, Corr D, Hinder S J (2007) Synthesis of High-Temperature Stable Anatase TiO_2 Photocatalyst. J. Phys. Chem. C. 111: 1605-1611.

[14] Kansal S K, Singh M, Sud D (2007) Studies on Photodegradation of Two Commercial Dyes in Aqueous Phase Using Different Photocatalysts. J. Hazard. Mater. 141: 581-590.

[15] Jiao T, Wang Y, Guo W, Zhang Q, Yan X, Chen J, Wang L, Xie D, Gao F (2012) Synthesis and Photocatalytic Property of Gold Nanoparticles by Using a Series of Bolaform Schiff Base Amphiphiles. Mater. Res. Bull. 47: 4203-4209.

[16] Kuo W S, Ho P H (2006) Solar Photocatalytic Decolorization of Dyes in Solution with TiO_2 Film. Dyes Pigments. 71: 212-217.

[17] Sakthivel S, Neppolian B, Shankar M V, Arabindoo B, Palanichamy M, Murugesan V (2003) Solar Photocatalytic Degradation of Azo Dye: Comparison of Photocatalytic Efficiency of ZnO and TiO_2. Sol. Energy Mater. Sol. Cells. 80: 65-82.

[18] Jiang Q, Zhang S C, Wang L Q, Liu C H (2006) Preparation of Perovskite Photocatalysts and Its Applications Progress. Chem. Ind. Eng. Prog. 25: 136-139.

[19] Ohno T, Tsubota T, Nakamura Y, Sayama K (2005) Preparation of S, C Cation-Codoped $SrTiO_3$ and Its Photocatalytic Activity Under Visible Light. Appl. Catal A-Gen. 288: 74-79.

[20] Lin X, Guan Q F, Zou C J, Liu T T, Zhang Y, Liu C B, Zhai H J (2013) Photocatalytic Degradation of An Azo Dye Using $Bi_{3.25}M_{0.75}Ti_3O_{12}$ Nanowires(M=La, Sm, Nd, and Eu). Mater. Sci. Eng. B. 178: 520-526.

[21] Liu H Y, Guo Y P, Guo B, Zhang D (2013) Synthesis and Visible-Light Photocatalysis Capability of $BiFeO_3$-$(Na_{0.5}Bi_{0.5})TiO_3$ Nanopowders by A Sol-gel Method. Solid State Sci. 19: 69-72.

[22] Hu J, Ma J H, Wang L N, Huang H (2014) Synthesis and Photocatalytic Properties of $LaMnO_3$-Graphene Nanocomposites. J. Alloys Comp. 583: 539-545.

[23] Shaterian M, Enhessari M, Rabbani D, Asghari M, Salavati-Niasari M (2014) Synthesis, Characterization and Photocatalytic Activity of $LaMnO_3$ Nanoparticles. Appl. Surf. Sci. Available: http://www.sciencedirect.com/science/article/pii/S0169433214006278. Accessed 2014 Mar 22.

[24] Naidu B S, Uttam G, Urmimala M, Rao C N R (2014) Visible Light Induced Oxidation of Water by Rare Earth Manganites, Cobaltites and Related Oxides. Chem. Phys. Lett. 591: 277-281.

[25] Cao Q M, Yu Q M, Connell D W, Yu G (2013) Titania/Carbon Nanotube Composite (TiO_2/CNT) and Its Application for Removal of Organic Pollutants. Clean Techn. Environ. Policy 15: 871-880.

[26] Baiju K V, Nada M D, Daniel F S, Wu J S, Kimberly A G (2012) Coupling Titania Nanotubes and Carbon Nanotubes To Create Photocatalytic Nanocomposites. ACS Catal. 2: 223-229.

[27] Gan Y P, Qin H P, Huang H, Tao X Y, Fang J W, Zhang W K (2013) Preparation and Photocatalytic Activity of Rutile TiO_2-Graphene Composites. Acta Phys. Chim. Sin. 29: 403-410.

[28] Wu J M, Yao J J, Yang H P, Fan Y I, Xu B L (2010). Photocatalytic Properties and the Role of Carbon Nanotubes in TiO_2/Carbon Nanotube Composites. Acta Chimica Sinica. 68: 1349-1356.

[29] Charlier J C (2002) Defects in Carbon Nanotubes. Acc. Chem. Res. 35: 1063-1069.

[30] Xian T, Yang H, Dai J F, Wei Z Q, Ma J Y, Feng W J (2011) Photocatalytic Properties of $SrTiO_3$ Nanoparticles Prepared by A Polyacrylamide Gel Route. Mater. Lett. 65: 3254-3257.